# Electric-Dipole Radiation over a Wedge with Imperfectly Conductive Faces: A First-Order Physical-Optics Solution

Athanasios I. Papadopoulos, *Student Member, IEEE*, and Dimitrios P. Chrissoulidis, *Member, IEEE*

***Abstract*—We solve a three-dimensional (3-D) electromagnetic diffraction problem involving an obtuse wedge with penetrable planar faces and an electric dipole which is parallel to the edge of the wedge. The analytical formulation is based on Stratton–Chu integrals of the electromagnetic field, which is excited by the dipole source on infinitely extending planes that coincide with the faces of the wedge. Fictitious charges are introduced along the edge to account for the discontinuity of the electromagnetic field on the faces across the edge. We evaluate asymptotically the integral expressions for the electric-field intensity far from the edge to obtain uniformly valid formulas. Our first-order physical-optics solution incorporates single reflection from both faces, the lateral wave, the edge-diffracted space wave, the edge-diffracted lateral wave, and transition terms which ensure that the electromagnetic field is finite and continuous at the single-reflection and lateral-wave boundaries. The numerical results establish the validity of this solution through a reciprocity check and comparisons with other analytical solutions.**

***Index Terms*—Diffraction by wedges, electromagnetic diffraction, electromagnetic scattering.**

## I. Introduction

ELECTROMAGNETIC (EM) wave scattering by penetrable wedges or corners is important in a variety of applications; consequently, it has attracted the interest of many researchers [1]–[24]. The surface impedance boundary condition (SIBC) is usually imposed on the wedge faces [1]–[18]; other approaches are based either on a heuristic extension of the perfect conductivity uniform theory of diffraction (UTD) [20]–[22] or on physical-optics (PO) approximations [23]–[25].

An exact solution to the scalar problem of plane wave scattering by an impedance wedge of arbitrary angle was given by Maliuzhinets [1] for the special case of normal incidence; the field, within the framework of the Maliuzhinets solution, is expressed as a Sommerfeld spectral integral. Tiberio *et al*. [2] obtained uniform far-field formulas by removal of the singularities of the asymptotic expressions given in [1]. The theory of [1] and [2], properly adapted to a wedge of arbitrary angle, was developed further by Griesser and Balanis [3], who obtained numerically efficient expressions. The response of a half-plane with two face impedances to plane wave and line-source excitation was determined by Sanyal and Bhattacharyya [4]. The case of line-source illumination of a generic impedance wedge was studied by Tiberio *et al*. [5] and Pelosi *et al*. [6], who derived asymptotic expressions for the edge-diffracted field; the source in these papers was assumed to be far from or at the edge of the wedge. Manara *et al*. [7] used the solution of [5] to derive asymptotic expressions for the surface wave components of the field. Recently, Otero and Rojas [8] used the solution of [1] to evaluate the line-source response of an impedance wedge with no restrictions on the location of the source or the field point.

When skew incidence is considered, the problem is rather involved and, therefore, only special cases had been treated [9]–[16] until recently. Pelosi *et al*. [17] employed an incremental-length diffraction coefficient formulation, which applies to impedance wedge problems possessing an explicit solution for the related Sommerfeld spectrum. Recently, Demeterscu [18] presented the exact solution to a diffraction problem involving an impedance wedge of arbitrary angle and an obliquely incident plane wave.

The SIBC is the starting point of the aforementioned papers. Alternatively, the UTD solution to diffraction by a perfectly conductive wedge [19] was heuristically modified [20]–[22] to account for finite conductivity and/or surface roughness. Furthermore, plane wave scattering by a dielectric wedge was studied [23]–[25] through a PO approximation based on a dual integral equation in the spectral domain.

In this paper, we present a first-order PO solution to the three-dimensional (3-D) problem of dipole radiation over a wedge with imperfectly conductive faces. Our solution can be applied to studies of mixed-path propagation of EM waves (e.g., over a coastal wedge). As yet, to the best of our knowledge, there is no exact solution to this 3-D problem. When point-source excitation is considered, the applicability of the SIBC is limited to strongly refractive media, such as metallic materials [26]. Hence, it is uncertain whether an extension of existing methods based on the SIBC to 3-D geometry would model efficiently wedge-type problems involving poor conductors such as dry land. The heuristic UTD can be applied to point-source excitation; although its predictions agree with those of other methods as well as with measurements [20], [22], [27], its applicability is questionable because it lacks a rigorous theoretical basis.

Our formulation is based on the Stratton–Chu integral equation [28]. The far-field solution for dipole radiation over

Manuscript received April 6, 1998; revised July 14, 1999.

The authors are with the Department of Electrical and Computer Engineering, Faculty of Technology, Aristotle University of Thessaloniki, GR-54006 Thessaloniki, Greece.

Publisher Item Identifier S 0018-926X(99)09943-3.

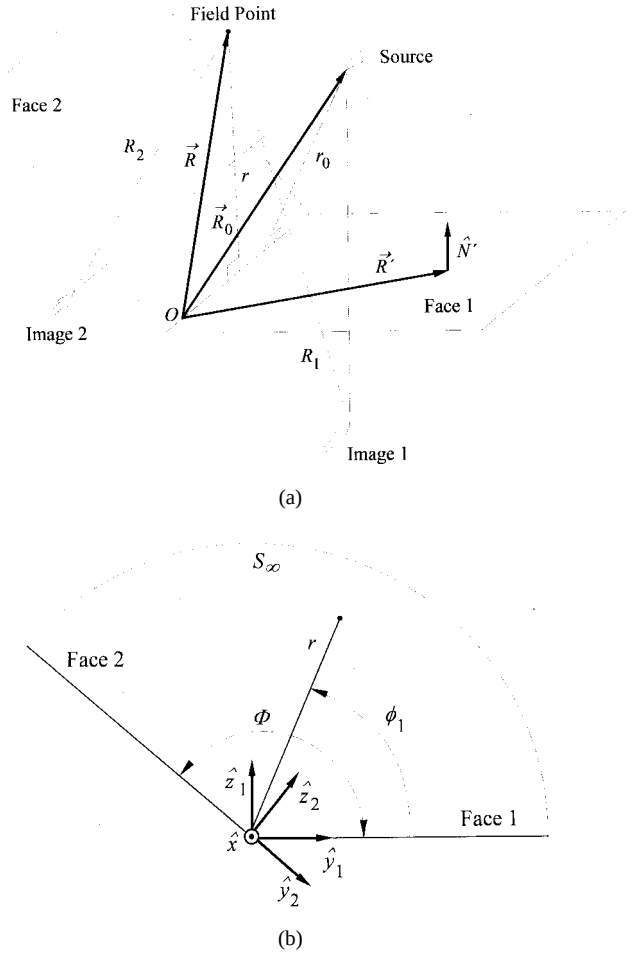


Fig. 1. Geometric configuration. (a) Electric dipole source, the images with respect to face 1 and face 2 and the arbitrary field point. (b) Side view.

a conductive half-space [29] serves as first-order approximation of the EM field on each face of the wedge. In order to compensate for the discontinuity of the field on the faces across the edge of the wedge, we introduce fictitious charges along the edge. The resulting integral expressions are asymptotically evaluated in the high-frequency regime. Thus, uniformly valid formulas are obtained, which allow for easy identification of the individual diffraction mechanisms. The edge-diffraction mechanism of our solution is augmented with an edge-diffracted lateral wave, the contribution of which is shown to be significant in some cases. The numerical results establish the validity and reveal several attractive features of our solution. We present a reciprocity check and comparisons with numerical results obtained through other analytical methods. Finally, we investigate the contribution of the edge-diffracted lateral wave to the total edge-diffracted field.

## II. Physical-Optics Formulation

The geometry of this radiation problem is presented in Fig. 1. Both faces of the wedge are planar and imperfectly conductive; $n_1$, $n_2$ is the (complex) refractive index of the medium under each face and $\Phi$ is the wedge angle. For the sake of analytical convenience, we introduce the Cartesian coordinate systems $(O;xy_1z_1)$ and $(O;xy_2z_2)$; the $x$-axis coincides with the edge, whereas the $z_1$- and $z_2$-axes are normal to the faces. Excitation is provided by an electric Hertz dipole, which is parallel to the edge of the wedge; the current density of this source is $\vec{J}(\vec{R}) = \vec{m}_e e^{j\omega t}\delta(\vec{R}-\vec{R}_0)$, where $\vec{m}_e = m_e\hat{x}$ is the electric dipole moment, $\vec{R}_0 = x_0\hat{x}+y_{0,i}\hat{y}_i+z_{0,i}\hat{z}_i$, and $i=1,2$. The harmonic time dependency $e^{j\omega t}$ is henceforth suppressed and, without loss of generality, we may use the normalization condition $m_e = j\omega\varepsilon_0$.

The scattered electric-field intensity above the wedge obeys the Stratton–Chu integral equation

$$\vec{E}^s(\vec{R}) = \oint_S [-j\omega\mu_0 G(\hat{N}'\times\vec{H}) + (\hat{N}'\times\vec{E}) \times\nabla' G + (\hat{N}'\cdot\vec{E})\nabla' G]\, ds' \tag{1}$$

where $S$ consists of face 1, face 2, and $S_\infty$ [Fig. 1(b)]; the latter connects the two faces through infinity; $\hat{N}'$ is the unit vector normal to $S$; $G(\vec{R}-\vec{R}') = e^{-jk_0|\vec{R}-\vec{R}'|}/4\pi|\vec{R}-\vec{R}'|$ is the free-space Green's function. Due to the radiation condition, the contribution to $\vec{E}^s$ from $S_\infty$ is zero. Therefore, $\vec{E}^s = \vec{E}^s_1 + \vec{E}^s_2$, where $\vec{E}^s_i$ represents the contribution of face $i$ to the scattered electric-field intensity.

The PO formulation of this paper is based on the assumption that the EM field on face $i$, which is a semi-infinite plane over a medium of refractive index $n_i$, is approximately the EM field that would be excited by the very same source on the corresponding, infinitely extending plane. Hence, according to [29], $\vec{E}$ and $\vec{H}$ on both faces can be expressed by use of Sommerfeld integrals in the spatial-frequency domain. If only high excitation frequencies are considered (i.e., $k_0R_i' \gg 1$), the electric-field intensity $\vec{E} = \vec{E}_i$ at any point $(x', y_i')$ on face $i$ can be expressed as the sum of a geometrical optics (GO) term and a lateral-wave (LW) term; thus, $\vec{E}_i = \vec{E}_i^{\rm GO} + \vec{E}_i^{\rm LW}$ on face $i$. The following expressions can be obtained for the terms $\vec{E}_i^{\rm GO}$, $\vec{E}_i^{\rm LW}$ of $\vec{E}_i$

$$\vec{E}_i^{\rm GO}(x', y_i') = \vec{e}_i^{\rm GO}(\varphi_i', \vartheta_i')\frac{e^{-jk_0R_i'}}{2\pi R_i'} \tag{2a}$$

$$\vec{E}_i^{\rm LW}(x', y_i') = \vec{e}_i^{\rm LW}(\varphi_i')\frac{e^{-jk_0R_i'\cos(\vartheta_i'-a_i)}}{2\pi\sqrt{\rho_i' R_i'^3\sin^3(\vartheta_i'-a_i)}} \times U(\vartheta_i'-\tilde{\vartheta}_i), \tag{2b}$$

where

$$\vec{e}_i^{\rm GO}(\varphi_i', \vartheta_i') = k_0^2\sin\vartheta_i'\cos\vartheta_i' \times\left[\hat{x}\frac{\sin\vartheta_i'\sin^2\varphi_i' + \cot\vartheta_i'\sqrt{n_i^2-\sin^2\vartheta_i'}}{n_i^2\cos\vartheta_i' + \sqrt{n_i^2-\sin^2\vartheta_i'}} - \frac{\hat{y}_i\sin\vartheta_i'\sin\varphi_i' - n_i^2\hat{z}_i\cos\vartheta_i'}{n_i^2\cos\vartheta_i' + \sqrt{n_i^2-\sin^2\vartheta_i'}}\cos\varphi_i'\right] \tag{3a}$$

$$\vec{e}_i^{\rm LW}(\varphi_i') = -\frac{jk_0}{n_i\sqrt{\cos a_i}}\left[\hat{x}\left(\sin^2\varphi_i' + n_i^2 - 1\right) - \hat{y}_i\sin\varphi_i'\cos\varphi_i' + \hat{z}_i n_i\cos a_i\cos\varphi_i'\right] \tag{3b}$$

$U(\cdot)$ is the unit-step function, $a_i = \sin^{-1} n_i$, $\tilde{\vartheta}_i = \mathrm{Re}\, a_i - \cos^{-1}(\mathrm{sech}(\mathrm{Im}\, a_i))$, and the variables $R_i'$, $\rho_i'$, $\varphi_i'$, $\vartheta_i'$ are defined as follows:

$$x' - x_0 = \rho_i' \cos\varphi_i' = R_i' \sin\vartheta_i' \cos\varphi_i' \tag{4a}$$

$$y_i' - y_{0,i} = \rho_i' \sin\varphi_i' = R_i' \sin\vartheta_i' \sin\varphi_i' \tag{4b}$$

$$z_{0,i} = R_i' \cos\vartheta_i'. \tag{4c}$$

The discontinuity of $\vec{E}_i^{\,\mathrm{LW}}(x', y_i')$ at $\vartheta_i' = \tilde{\vartheta}_i$, which may falsely be interpreted as an end-point contribution, is avoided by use of the following continuous expression:

$$\vec{E}_i^{\,\mathrm{LW}}(x', y_i') = \vec{e}_i^{\,\mathrm{LW}}(\varphi_i') \frac{e^{-jk_0 R_i' \cos(\vartheta_i' - a_i)}}{2\pi\sqrt{\rho_i' R_i'^3 \sin^3(\vartheta_i' - a_i)}} g(\vartheta_i') \tag{5}$$

which is equivalent to that of (2b); a proof of (5) and the definition of $g(\vartheta_i')$ are given in the Appendix. Expressions similar to those of (2a) and (5) can be obtained for the corresponding terms $\vec{H}_i^{\,\mathrm{GO}}$, $\vec{H}_i^{\,\mathrm{LW}}$ of the magnetic-field intensity $\vec{H}_i$ on face $i$, wherein

$$\begin{aligned}
&\vec{h}_i^{\,\mathrm{GO}}(\varphi_i', \vartheta_i') \\
&\quad = \omega\varepsilon_0 k_0 \cos\vartheta_i' \Bigg[ \hat{x} \sin^2\vartheta_i' \sin\varphi_i' \cos\varphi_i' \\
&\qquad \times \frac{\cos\vartheta_i' - \sqrt{n_i^2 - \sin^2\vartheta_i'}}{n_i^2 \cos\vartheta_i' + \sqrt{n_i^2 - \sin^2\vartheta_i'}} \\
&\qquad - \hat{y}_i \frac{n_i^2 \cos\vartheta_i' - \sin^2\vartheta_i' \sin^2\varphi_i' (\cos\vartheta_i' - \sqrt{n_i^2 - \sin^2\vartheta_i'})}{n_i^2 \cos\vartheta_i' + \sqrt{n_i^2 - \sin^2\vartheta_i'}} \\
&\qquad - \hat{z}_i \frac{\sin\vartheta_i' \sin\varphi_i'}{\cos\vartheta_i' + \sqrt{n_i^2 - \sin^2\vartheta_i'}} \Bigg]
\end{aligned} \tag{6a}$$

$$\begin{aligned}
&\vec{h}_i^{\,\mathrm{LW}}(\varphi_i') \\
&\quad = \frac{\omega\varepsilon_0\sqrt{\cos a_i}}{j n_i} \Big[ \hat{x}\big(n_i^2 + 1\big) \sin\varphi_i' \cos\varphi_i' \\
&\qquad - \hat{y}_i \big(1 - \big(n_i^2 + 1\big) \sin^2\varphi_i'\big) - \hat{z}_i \frac{n_i^3 \sin\varphi_i'}{\cos a_i} \Big]
\end{aligned} \tag{6b}$$

must be used instead of $\vec{e}_i^{\,\mathrm{GO}}$ and $\vec{e}_i^{\,\mathrm{LW}}$, respectively.

It is an essential part of our approach that LW terms are taken into account when the dipole is over face $i$, which is equivalent to the condition $(-1)^i y_{0,i} < 0$; if the latter is not true, $\vec{E}_i^{\,\mathrm{LW}}$ and $\vec{H}_i^{\,\mathrm{LW}}$ are ignored. Since, generally, GO and LW terms coexist, (1) yields

$$\vec{E}_i^{\,s} = \iint_{\mathrm{face}\, i} \frac{e^{-jk_0 R_i''}}{8\pi^2 R_i' R_i''^2} \Big[ \vec{F}_i^{\,\mathrm{GO}}(\vec{R}') e^{-jk_0 R_i'} + \vec{F}_i^{\,\mathrm{LW}}(\vec{R}') \frac{e^{-jk_0 R_i' \cos(\vartheta_i' - a_i)}}{\sqrt{\rho_i' R_i' \sin^3(\vartheta_i' - a_i)}} g(\vartheta_i') \Big] \, ds' \tag{7}$$

where $R_i'' = \sqrt{(x - x')^2 + (y_i - y_i')^2 + z_i^2}$ and

$$\begin{aligned}
&(jk_0)^{-1} \vec{F}_i^{\,\gamma}(\vec{R}') \\
&\quad = \hat{x} \big[ z_i e_{i,x}^{\gamma} + R''_i Z_0 h_{i,y}^{\gamma} + (x - x') e_{i,z}^{\gamma} \big] \\
&\qquad - \hat{y}_i \big[ R''_i Z_0 h_{i,x}^{\gamma} - z_i e_{i,y}^{\gamma} - (y_i - y_i') e_{i,z}^{\gamma} \big] \\
&\qquad - \hat{z}_i \big[ (x - x') e_{i,x}^{\gamma} + (y_i - y_i') e_{i,y}^{\gamma} - z_i e_{i,z}^{\gamma} \big]
\end{aligned} \tag{8}$$

the superscript $\gamma$ standing for GO or LW; $Z_0 = \sqrt{\mu_0/\varepsilon_0}$ is the intrinsic impedance of free space. As only high frequencies are considered, both terms in the right-hand side of (7), hereinafter denoted as $\vec{E}_i^{\,s,\mathrm{GO}}$ and $\vec{E}_i^{\,s,\mathrm{LW}}$, can be evaluated asymptotically through use of the modified steepest-descent method (SDM) [31], which allows for saddle points to be near the end-points of the integration path.

The Cartesian coordinates $x'$, $y_i'$ are convenient integration variables for the evaluation of $\vec{E}_i^{\,s,\mathrm{GO}}$

$$\vec{E}_i^{\,s,\mathrm{GO}} = \pm \int_0^{\pm\infty} \left\{ \int_{-\infty}^{\infty} \vec{F}_i^{\,\mathrm{GO}}(\vec{R}') \frac{e^{-jk_0(R_i' + R_i'')}}{8\pi^2 R_i' R_i''^2} \, dx' \right\} dy_i'. \tag{9}$$

Upper and lower signs in (9) correspond to $i = 1$ and $i = 2$, respectively. The presence of $R_i'$, $R_i''$ in the integrand gives rise to four branch-point singularities in the complex $x'$-plane and the complex $y_i'$-plane. The corresponding branch cuts are drawn along $\mathrm{Im}\, R_i' = 0$ and $\mathrm{Im}\, R_i'' = 0$. The contours of integration are properly indented so that they lie in the Riemann surface with $\mathrm{Im}\, R_i' < 0$ and $\mathrm{Im}\, R_i'' < 0$. By application of the modified SDM to the integral over $x'$ and then to the integral over $y_i'$, we derive the following high-frequency expression:

$$\begin{aligned}
\vec{E}_i^{\,s,\mathrm{GO}} &\approx \frac{\vec{F}_i^{\,\mathrm{GO}}\big(\vec{R}_{i,\mathrm{sp}}^{\,\mathrm{GO}}\big) e^{-jk_0 R_i}}{4\pi j k_0 R_i z_i} U((-1)^i(\phi_i + \phi_{0,i} - \pi)) \\
&\quad + \frac{(-1)^i r_0 \vec{F}_i^{\,\mathrm{GO}}\big(\vec{R}_{\mathrm{ep}}^{\,\mathrm{GO}}\big) e^{-jk_0 D}}{4\pi j k_0 (r y_{0,i} + r_0 y_i)\sqrt{2\pi j k_0 r r_0 D}} \\
&\quad - \frac{\vec{F}_i^{\,\mathrm{GO}}\big(\vec{R}_{i,\mathrm{sp}}^{\,\mathrm{GO}}\big) e^{-jk_0 D}}{8\pi j k_0 R_i z_i} \, \mathrm{sgn}((-1)^i(\phi_i + \phi_{0,i} - \pi)) \\
&\quad \times [f(\sqrt{k_0 |R_i - D|/2}) - 1/\sqrt{j\pi k_0 |R_i - D|}]
\end{aligned} \tag{10}$$

where $\vec{R}_{i,\mathrm{sp}}^{\,\mathrm{GO}} = (\hat{x}(x_0 z_i + x z_{0,i}) + \hat{y}_i(y_{0,i} z_i + y_i z_{0,i}))/(z_i + z_{0,i})$, $\vec{R}_{\mathrm{ep}}^{\,\mathrm{GO}} = (x_0 r + x r_0)\hat{x}/(r + r_0)$, $R_i^2 = (x - x_0)^2 + (y_i - y_{0,i})^2 + (z_i + z_{0,i})^2$, $D^2 = (x - x_0)^2 + (r + r_0)^2$, and $y_i = r\cos\phi_i$, $z_i = r\sin\phi_i$, $y_{0,i} = r_0\cos\phi_{0,i}$, $z_{0.i} = r_0\sin\phi_{0,i}$; $f(\xi) = e^{2j\xi^2}\mathrm{erfc}(\xi + j\xi)$. The first term in the right-hand side of (10) is the contribution of the saddle point to the integral; it represents the singly-reflected field from face $i$, which is discontinuous across the corresponding single reflection boundary (RB). The second term is the end-point contribution; it represents the edge-diffracted field, which is infinite along the RB. The third term eliminates the singularities of the other terms, thus leading to a uniformly valid expression for $\vec{E}_i^{\,s,\mathrm{GO}}$. Far from the RB, the third term is insignificant and, therefore, it may be ignored.

We follow a slightly different procedure for the asymptotic evaluation of $\vec{E}_i^{\,s,\mathrm{LW}}$, which may be written as $\vec{E}_i^{\,s,\mathrm{LW}} =$

$\vec{E}^{s,\mathrm{LW}}_{i,\rho\varphi}+\vec{E}^{s,\mathrm{LW}}_{i,xy}$. Each of these terms is expressed as a double integral:

$$\vec{E}^{s,\mathrm{LW}}_{i,\rho\varphi}=e^{-jk_0z_{0,i}\cos a_i}\int_0^{\infty}\left\{\int_0^{2\pi}\vec{F}^{\mathrm{LW}}_i(\vec{R}')\frac{e^{-jk_0R''_i}}{8\pi^2R''^2_i}\,d\varphi'_i\right\}\times\frac{g(\vartheta'_i)\sqrt{\rho'_i}e^{-jn_ik_0\rho'_i}}{\sqrt{(\rho'_i\cos a_i-n_iz_{0,i})^3}}\,d\rho'_i \tag{11a}$$

$$\vec{E}^{s,\mathrm{LW}}_{i,xy}=\mp e^{-jk_0z_{0,i}\cos a_i}\int_{\mp\infty}^{0}\left\{\int_{-\infty}^{\infty}\vec{F}^{\mathrm{LW}}_i(\vec{R}')\times\frac{g(\vartheta'_i)e^{-jk_0(R''_i+n_i\rho'_i)}}{8\pi^2R''^2_i\sqrt{\rho'_i(\rho'_i\cos a_i-n_iz_{0,i})^3}}\,dx'\right\}dy'_i. \tag{11b}$$

Upper and lower signs in (11b) correspond to $i=1$ and $i=2$, respectively. When applying SDM to (11a), we account for the branch points introduced by $R''_i$, the corresponding branch cuts are along $\mathrm{Im}\,R''_i=0$, and the contour of integration is properly indented so as to lie in the Riemann surface $\mathrm{Im}\,R''_i<0$. The presence of branch cuts in the complex $\varphi'_i$-plane has no effect on the integral over $\varphi'_i$, as calculated by SDM, because the steepest-descent contour (SDC) through the saddle points $\varphi_i$ and $\varphi_i\pm\pi$ does not intersect the branch cuts. As regards the integral over $\rho'_i$, we apply SDM with respect to the saddle point $\rho_i-z_i\tan a_i$, which is in the Riemann surface $\mathrm{Im}\,R''_i>0$. The end-result is the following asymptotic expression for $\vec{E}^{s,\mathrm{LW}}_{i,\rho\varphi}$:

$$\vec{E}^{s,\mathrm{LW}}_{i,\rho\varphi}\approx\frac{\vec{F}^{\mathrm{LW}}_i(\vec{R}^{\mathrm{LW}}_{i,\mathrm{sp}})e^{-jk_0(n_i\rho_i+(z_i+z_{0,i})\cos a_i)}}{8\pi jk_0z_i\sqrt{\rho_i(\rho_i\cos a_i-n_i(z_i+z_{0,i}))^3}}\times\left[2U(\vartheta_i-\tilde{\vartheta}_i)+(f(\tilde{\xi}_i)\,\mathrm{sgn}(\tilde{\vartheta}_i-\vartheta_i)-1/\tilde{s}_i\sqrt{\pi k_0})e^{-k_0\tilde{s}_i^2}\right] \tag{12}$$

where $\vec{R}^{\mathrm{LW}}_{i,\mathrm{sp}}=(x_0+(\rho_i-z_i\tan a_i)\cos\varphi_i)\hat{x}+(y_{0,i}+(\rho_i-z_i\tan a_i)\sin\varphi_i)\hat{y}_i$, $\tilde{\rho}_i=z_{0,i}\tan\tilde{\vartheta}_i$, $\tilde{R}_i^2=(\tilde{\rho}_i-\rho_i)^2+z_i^2$, $\tilde{s}_i^2=-j(n_i(\rho_i-\tilde{\rho}_i)+z_i\cos a_i-\tilde{R}_i)$, and $\tilde{\xi}_i=\tilde{s}_i\sqrt{k_0/2j}\,\mathrm{sgn}(\tilde{\vartheta}_i-\vartheta_i)$. Similar asymptotic evaluation of $\vec{E}^{s,\mathrm{LW}}_{i,xy}$ yields (13), shown at the bottom of the next page, where $\vec{R}^{\mathrm{LW}}_{i,\mathrm{ep}}=x'_{i,s}\hat{x}$, $\rho'^2_{i,s}=(x'_{i,s}-x_0)^2+y^2_{0,i}$, $R'^2_{i,s}=\rho'^2_{i,s}+z^2_{0,i}$, $R''^2_{i,s}=(x'_{i,s}-x)^2+r^2$; $\vartheta'_{i,s}=\sin^{-1}(\rho'_{i,s}/R'_{i,s})$, $s_i^2=-j(n_i(\rho_i-\rho'_{i,s})+z_i\cos a_i-R''_{i,s})$, $\xi_i=s_i\sqrt{k_0/2j}\,\mathrm{sgn}(\mathrm{Re}\,s_i)$; $x'_{i,s}$ is determined from the equation $n_i(x'_{i,s}-x_0)/\rho'_{i,s}+(x'_{i,s}-x)/R''_{i,s}=0$, which is solved numerically; the appropriate solution must conform to the restrictions $\mathrm{Re}\{n_i\rho'_{i,s}+R''_{i,s}\}>0$ and $\mathrm{Im}\{n_i\rho'_{i,s}+R''_{i,s}\}\le 0$, which ensure that the radiation condition is satisfied. In the special case $x=x_0$, though, it is readily verified that $x_{i,s}=x$. Adding (12) and (13), we obtain (14), shown at the bottom of the page. The first term in the right-hand side of (14) is the lateral wave on face $i$; the second term is the edge-diffracted lateral wave, the contribution of which to the total edge-diffracted field is examined in Section IV. The remaining transition terms in the right-hand side of (14) ensure the continuity of the field across the boundaries of the region wherein the lateral wave is present.

## III. Correction to Physical-Optics Solution

Up to this point, though, the analytical formulation has the drawback that the field on the faces is discontinuous across the edge. In order to account for this discontinuity, additional terms must be included in the right-hand side of (1).

We consider the auxiliary geometry of Fig. 2, wherein both faces of the wedge acquire the shape of a cylindrical surface near the edge; let $a$ be the radius of that cylindrical surface. According to the surface equivalence theorem [28], the field

$$\vec{E}^{s,\mathrm{LW}}_{i,xy}\approx\frac{j\vec{F}^{\mathrm{LW}}_i(\vec{R}^{\mathrm{LW}}_{i,\mathrm{sp}})e^{-jk_0(n_i\rho_i+(z_i+z_{0,i})\cos a_i)}}{8\pi k_0z_i\sqrt{\rho_i(\rho_i\cos a_i-n_i(z_i+z_{0,i}))^3}}\left[2U((-1)^{i+1}\mathrm{Re}\,s_i)+(-1)^i\big(f(\xi_i)\,\mathrm{sgn}(\mathrm{Re}\,s_i)-1/s_i\sqrt{\pi k_0}\big)e^{-k_0s_i^2}\right]+\frac{(-1)^i\vec{F}^{\mathrm{LW}}_i(\vec{R}^{\mathrm{LW}}_{i,\mathrm{ep}})\rho'^2_{i,s}e^{-jk_0z_{0,i}\cos a_i}g(\vartheta'_{i,s};R'_{i,s})\sqrt{2jR''_{i,s}}e^{-jk_0(n_i\rho'_{i,s}+R''_{i,s})}}{8\pi k_0\big(n_iy_{0,i}R''_{i,s}+y_i\rho'_{i,s}\big)\sqrt{\pi k_0\big(n_iy^2_{0,i}R''^3_{i,s}+r^2\rho'^3_{i,s}\big)(\rho'_{i,s}\cos a_i-n_iz_{0,i})^3}} \tag{13}$$

$$\begin{aligned}\vec{E}^{s,\mathrm{LW}}_i\approx{}&\frac{\vec{F}^{\mathrm{LW}}_i(\vec{R}^{\mathrm{LW}}_{i,\mathrm{sp}})e^{-jk_0(n_i\rho_i+(z_i+z_{0,i})\cos a_i)}}{4\pi jk_0z_i\sqrt{\rho_i(\rho_i\cos a_i-n_i(z_i+z_{0,i}))^3}}\left[U(\vartheta_i-\tilde{\vartheta}_i)-U((-1)^{i+1}\mathrm{Re}\,s_i)\right]\\&+\frac{(-1)^i\vec{F}^{\mathrm{LW}}_i(\vec{R}^{\mathrm{LW}}_{i,\mathrm{ep}})\rho'^2_{i,s}e^{-jk_0(n_i\rho'_{i,s}+z_{0,i}\cos a_i+R''_{i,s})}g(\vartheta'_{i,s};R'_{i,s})\sqrt{2jR''_{i,s}}}{8\pi k_0(n_iy_{0,i}R''_{i,s}+y_i\rho'_{i,s})\sqrt{\pi k_0\big(n_iy^2_{0,i}R''^3_{i,s}+r^2\rho'^3_{i,s}\big)(\rho'_{i,s}\cos a_i-n_iz_{0,i})^3}}\\&+\frac{\vec{F}^{\mathrm{LW}}_i(\vec{R}^{\mathrm{LW}}_{i,\mathrm{sp}})e^{-jk_0(n_i\tilde{\rho}_i+z_{0,i}\cos a_i+\tilde{R}_i)}}{8\pi jk_0z_i\sqrt{\rho_i(\rho_i\cos a_i-n_i(z_i+z_{0,i}))^3}}[f(\tilde{\xi}_i)\,\mathrm{sgn}(\tilde{\vartheta}_i-\vartheta_i)-1/\tilde{s}_i\sqrt{\pi k_0}]\\&-\frac{(-1)^i\vec{F}^{\mathrm{LW}}_i(\vec{R}^{\mathrm{LW}}_{i,\mathrm{sp}})e^{-jk_0(n_i\rho'_{i,s}+z_{0,i}\cos a_i+R''_{i,s})}}{8\pi jk_0z_i\sqrt{\rho_i(\rho_i\cos a_i-n_i(z_i+z_{0,i}))^3}}[f(\xi_i)\,\mathrm{sgn}(\mathrm{Re}\,s_i)-1/s_i\sqrt{\pi k_0}]\end{aligned} \tag{14}$$

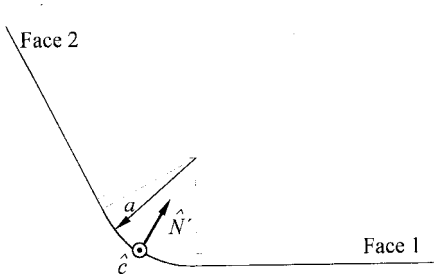


Fig. 2. Auxiliary geometry in the vicinity of the edge $C$.

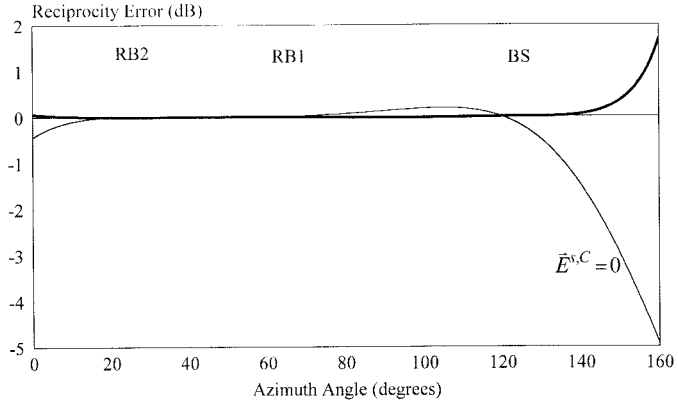


(a)

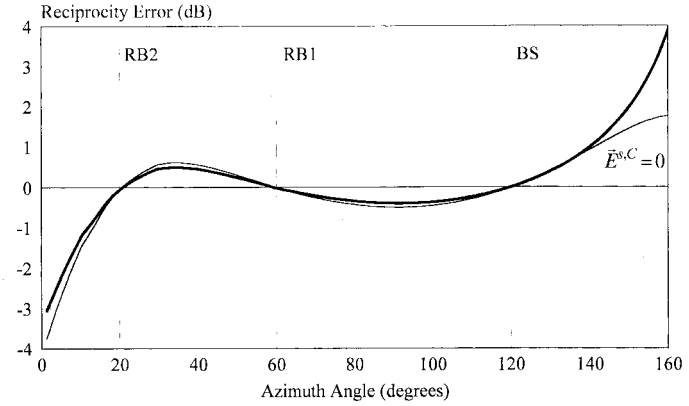


(b)

Fig. 3. Reciprocity error of the edge-diffracted part of the field: $|E_x^d(\vec{R};\vec{R}_0)|/|E_x^d(\vec{R}_0;\vec{R})|$ versus $\phi_1(x = x_0 - 100\text{ m},\ r = 50\text{ m},\ r_0 = 100\text{ m},\ \phi_{0,1} = 120^\circ,\ \Phi = 160^\circ)$. (a) Land and (b) coastal wedge.

above the wedge, thus smoothened, is identical to that radiated by an equivalent electric current $\vec{J}_{\rm eq} = \hat{N}' \times \vec{H}$ and an equivalent magnetic current $\vec{M}_{\rm eq} = -\hat{N}' \times \vec{E}$ on the faces. If the field on each face is approximated independently (as in Section II) the aforementioned equivalent surface currents will be discontinuous across line $C$, where the two faces meet (Fig. 2); therefore, Maxwell's equations will not hold there, unless fictitious charges are considered on $C$. The discontinuity of $\vec{J}_{\rm eq}$ gives rise to an electric charge along $C$, the line density of which is $\rho_\ell = \hat{c} \cdot [\vec{H}_2 - \vec{H}_1]_C / j\omega$ [30]. By the same token, the discontinuity of $\vec{M}_{\rm eq}$ gives rise to a magnetic charge along

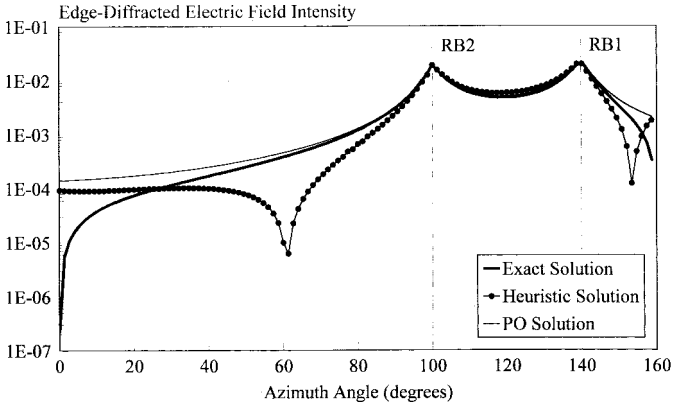


(a)

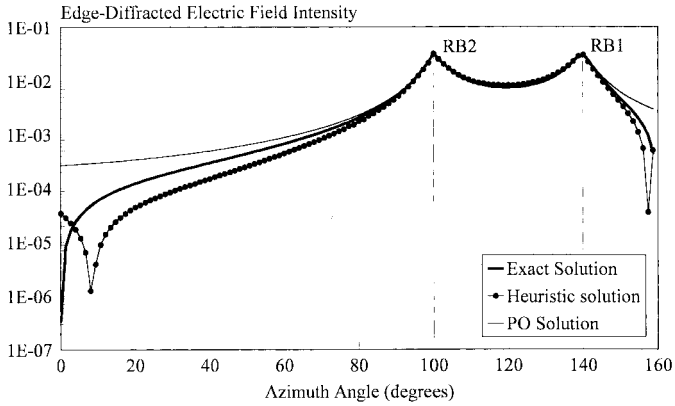


(b)

Fig. 4. Edge-diffracted electric-field intensity over land wedge: $|\vec{E}^d|$ versus $\phi_1(x = x_0,\ r = 20\text{ m},\ r_0 = 400\text{ m},\ \phi_{0,1} = 40^\circ,\ \Phi = 160^\circ)$. (a) Dry and (b) wet land faces.

$C$, its line density being $\sigma_\ell = \hat{c} \cdot [\vec{E}_1 - \vec{E}_2]_C / j\omega$. As the latter does not contribute to the scattered electric-field intensity, we only need to consider $\rho_\ell$.

In the limit $a \to 0$, which corresponds to the sharp wedge of Fig. 1, $\rho_\ell \to \hat{x} \cdot (\vec{H}_2(x', 0) - \vec{H}_1(x', 0))/j\omega$. This line charge contributes to $\vec{E}^s$ as follows:

$$\vec{E}^{s,C} = \frac{1}{\varepsilon_0} \int_C \rho_\ell \nabla' G \, d\ell' \tag{15}$$

and after some algebra it is proved that $\vec{E}^{s,C} = \vec{E}_2^{s,C} - \vec{E}_1^{s,C}$, where

$$\vec{E}_i^{s,C} = \int_{-\infty}^{\infty} \left[ \left( \vec{F}_{\ell,i}^{\rm GO}(\vec{R}') + \vec{F}_{\ell,i}^{\rm LW}(\vec{R}') g(\vartheta_i') \times \frac{e^{jk_0 R_i'(1-\cos(\vartheta_i' - a_i))}}{\sqrt{\rho_i' R_i' \sin^3(\vartheta_i' - a_i)}} \right) \frac{e^{-jk_0(R_i' + R_i'')}}{8\pi^2 R_i' R_i''^2} \right]_{y_i'=0} dx' \tag{16}$$

and $\vec{F}_{\ell,i}^{\gamma}(\vec{R}') = k_0 h_{i,x}^{\gamma}((x - x')\hat{x} + (y_i - y_i')\hat{y}_i + z_i \hat{z}_i)/\omega\varepsilon_0$. Asymptotic evaluation of the integrals in (16) yields the following high-frequency expression for $\vec{E}_i^{s,C}$ (see (17) at the bottom of the page). Thus, everything included, $\vec{E}^s =$

$\vec{E}_1^{s,\mathrm{GO}} + \vec{E}_2^{s,\mathrm{GO}} + \vec{E}_1^{s,\mathrm{LW}} + \vec{E}_2^{s,\mathrm{LW}} + \vec{E}^{s,C}$ is the scattered electric-field intensity from the wedge.

## IV. Numerical Results

Our solution was first checked with respect to the principle of reciprocity, according to which the component of the scattered electric-field intensity in the direction of the dipole axis must be unaffected by an interchange of the field and source positions. Hence, $E_x^s(\vec{R};\vec{R}_0) = E_x^s(\vec{R}_0;\vec{R})$ should hold for any pair of position vectors $\vec{R}$, $\vec{R}_0$ [Fig. 1(a)]. The GO singly-reflected wave from and the lateral wave on either face, which are represented by the first term in the right-hand side of (10) and (14), respectively, obviously satisfy reciprocity. The remaining, edge-diffracted, part of $\vec{E}^s$, which is herein denoted as $\vec{E}^d$, can only be checked numerically. Moreover, we examine the effect of the correction term $\vec{E}^{s,C}$ on the reciprocity error. The numerical results correspond to a land-sea (i.e., coastal) wedge and a land–land wedge; we used the refractive indices $n_s = 9.73 - j3.69$ and $n_l = 2.24 - j4.02 \times 10^{-3}$ for sea and (dry) land, respectively. The excitation frequency is $f = 1$ GHz.

Plots of $|E_x^d(\vec{R};\vec{R}_0)|/|E_x^d(\vec{R}_0;\vec{R})|$, which must be equal to one (i.e., 0 dB) for an exact solution, are presented in Fig. 3; the azimuth angle $\phi_1$ of the field point $\vec{R}$, which is at constant distance $r$ from the edge, varies in the range $(0, \Phi)$. Deviations of $|E_x^d(\vec{R};\vec{R}_0)|/|E_x^d(\vec{R}_0;\vec{R})|$ from the aforementioned reference level represent the reciprocity error of the edge-diffracted part of the field for the specific pair of positions $\vec{R}$, $\vec{R}_0$. Numerical results obtained without the correction term $\vec{E}^{s,C}$ are also presented. The reciprocity error is negligible in the vicinity of the single reflection boundaries RB1 and RB2 and it is equal to zero in the backscattering direction BS. In the case of the sloping land wedge [Fig. 3(a)] the reciprocity error of the uncorrected edge-diffracted field is less than 0.2 dB in most directions. Addition of the correction term $\vec{E}^{s,C}$ results in further reduction of the reciprocity error, which is thus kept small even close to the faces, where the first-order PO solution deteriorates. Similar remarks may accompany the numerical results for the coastal wedge [Fig. 3(b)]: compared to the previous case, the reciprocity error is slightly greater and yet it is less than 0.5 dB in most directions; if $\vec{E}^{s,C}$ is taken into account, though, the reciprocity error may increase in directions near a face of the wedge.

We next investigate a special scattering geometry, which allows for comparisons of our PO solution to a rigorous solution [1]–[3] and to a heuristic UTD solution [22]. The dipole source and the field point are both on the same $x$-plane (i.e., $x = x_0$), but $r_0 \gg r$, which is approximately the case of a plane wave normally incident upon the edge of the wedge. A sloping land wedge (Fig. 4) as well as a flat coastal wedge (Fig. 5) are considered. Results for dry land, with refractive index as above and wet land with $n_l = 5.47 - j3.28 \times 10^{-2}$ at $f = 1$ GHz, are presented in both cases. The surface impedance of the faces required for the exact solution is determined from $Z_i = Z_0/\sqrt{n_i^2 - \cos^2\phi_{0,i}}$.

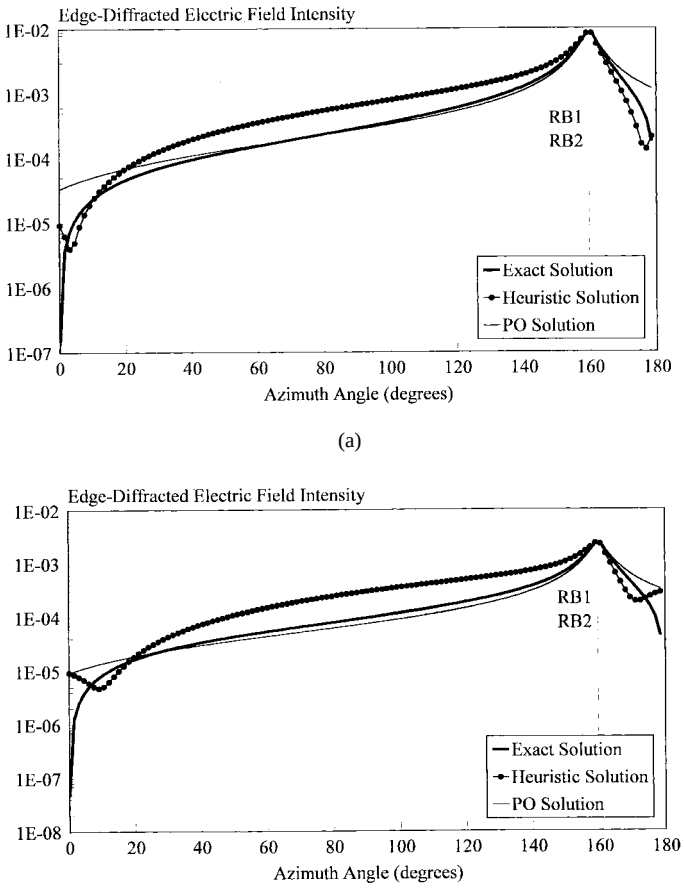


Fig. 5. Edge-diffracted electric-field intensity over coastal wedge: $|\vec{E}^d|$ versus $\phi_1 (x = x_0, r = 20\ \mathrm{m}, r_0 = 400\ \mathrm{m}, \phi_{0,1} = 20^\circ, \Phi = 180^\circ)$. (a) Dry and (b) wet land face.

The plots of $|\vec{E}^d|$ versus $\phi_1$ indicate that, generally, our PO solution is more accurate than the heuristic UTD solution. The latter deviates from the exact solution, especially when the nulls of the heuristic diffraction coefficient do not coincide with the faces of the wedge. In the case of the sloping land wedge (Fig. 4), the heuristic UTD solution improves as $|n_l|$ increases seemingly because the nulls approach the faces of the wedge. This trend is disproved in the case of the coastal wedge (Fig. 5), where the nulls are very close to the faces for both values of $n_l$. The inconsistent behavior of the heuristic UTD solution for increasing $|n_l|$ raises questions about its accuracy and its limit of applicability. On the other hand, our PO solution is in very good agreement with the exact solution in a wide range of scattering directions; discrepancies are observed

$$\vec{E}_i^{s,C} \approx \frac{\vec{F}_{\ell,i}^{\mathrm{GO}}(\vec{R}_{\mathrm{ep}}^{\mathrm{GO}})(r+r_0)e^{-jk_0D}}{4\pi rD\sqrt{2\pi jk_0rr_0D}} + \frac{\vec{F}_{\ell,i}^{\mathrm{LW}}(\vec{R}_{i,\mathrm{ep}}^{\mathrm{LW}})\rho'_{i,s}e^{-jk_0(n_i\rho'_{i,s}+z_{0,i}\cos a_i+R''_{i,s})}g(\vartheta'_{i,s};R'_{i,s})}{4\pi\sqrt{2\pi jk_0R''_{i,s}\left(n_iy_{0,i}^2R''^3_{i,s}+r^2\rho'^3_{i,s}\right)(\rho'_{i,s}\cos a_i - n_iz_{0,i})^3}} \tag{17}$$

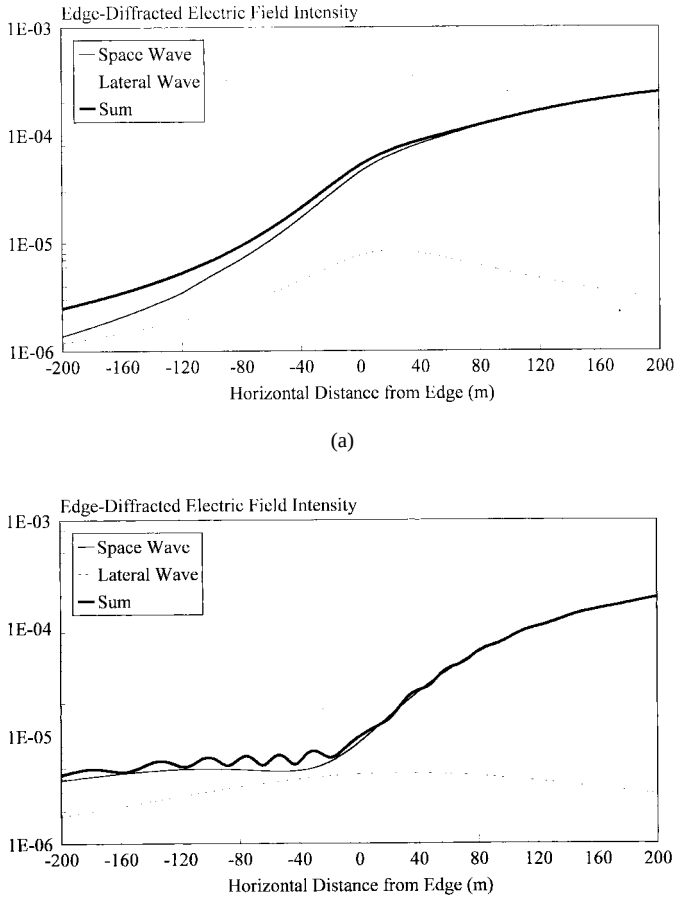


Fig. 6. Edge-diffracted electric-field intensity at constant altitude over land-land wedge: $|\vec{E}^d|$ versus $y_1 (z_1 = 50$ m, $y_{0,1} = -5$ m, $z_{0,1} = 0.05$ m, $\Phi = 180^\circ)$. (a) $x - x_0 = 0$. (b) $x - x_0 = 150$ m.

when the field point is close to a face, regardless of the wedge angle and of the refractive index of the medium under each face. Still, our PO solution consistently provides more accurate numerical results than the heuristic UTD solution, as long as the field point is not very close to the faces.

Finally, we investigate the contribution of the edge-diffracted lateral wave to the total edge-diffracted field. The lateral wave is usually ignored by other solutions, such as the heuristic UTD solution discussed above; this is justifiable, up to a point because if $|n_i| > 1$, the GO currents on the faces are generally stronger than the LW currents and, therefore, space-wave diffraction dominates over lateral-wave diffraction. Yet, there are special cases (e.g., the source being very close to a face and not very far from the edge), which allow for the two diffraction mechanisms to be comparable. We examine two such cases next (Fig. 6): the magnitude of the electric-field intensity associated with the edge-diffracted space wave and the edge-diffracted lateral wave and both are plotted versus the horizontal distance $y_1$ from the edge at constant altitude above a nonsloping land wedge. The left-hand face of the wedge represents fertile land $(n_1 = 3.16 - j2.84 \times 10^{-2})$, the right-hand face represents dry land $(n_2 = 2.24 - j4.02 \times 10^{-3})$, and the source is over the latter. The constant altitude $z_1$ is chosen so that the field point is not very close to either face of

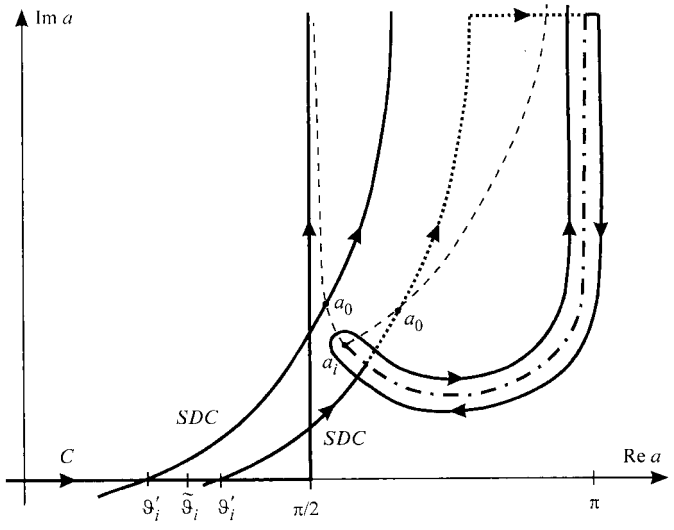


Fig. 7. Contour deformation in the complex $a$-plane; the steepest-descent contour is shown for $\vartheta_i' = \vartheta_i^-$ and $\vartheta_i' = \vartheta_i^+$.

the flat wedge. Evidently, if the source and the field point are over the same face, both diffraction mechanisms must be taken into account. If $x \neq x_0$ [Fig. 6(b)], an interference pattern is present on the plot of the total edge-diffracted electric-field intensity; this pattern is attributed to the phase difference of the two edge-diffracted waves, which is not independent of $y_1$ in this case.

## V. Conclusion

This paper presents a first-order PO solution to the 3-D problem of electric dipole radiation in the presence of a wedge with penetrable planar faces. In its present form, the theory applies to a dipole that is parallel to the edge, the discontinuity of the surface EM field across the edge is taken into account, and interactions between the two faces are neglected. The integral expressions for the scattered electric-field intensity are evaluated asymptotically by use of the steepest-descent method. The resulting solution accounts for the GO singly-reflected waves, the lateral wave, the edge-diffracted space wave, and the edge-diffracted lateral wave. The latter may be an important diffraction mechanism under certain conditions. Our solution also includes transition terms, which ensure that the EM field is finite and continuous at the single-reflection boundaries and the lateral-wave boundaries. Reciprocity is satisfied, especially when a heuristic correction term is included. Accurate results are obtained whenever multiple-reflection mechanisms are negligible or nonexistent, provided that the field point is not very close to either face of the wedge. The analytical formulation of this paper is currently extended to deal with excitation by arbitrarily oriented electric or magnetic dipoles and with problems of wave propagation over a ridge in hilly or mountainous terrain.

## Appendix

The analytical procedure toward a closed-form expression for the dipole radiation over a conductive half space involves

the asymptotic evaluation of the integral

$$I(\vartheta_i') = \int_C F(a) e^{-jk_0 R_i' \cos(\vartheta_i' - a)}\, da \tag{18}$$

where $C$ extends from $-\pi/2 - j\infty$ to $\pi/2 + j\infty$ and $F(\alpha)$ has a branch-point singularity of the type $\sqrt{n_i^2 - \sin^2 a}$ (Fig. 7). By application of the standard SDM, $I(\vartheta_i')$ is approximated as follows:

$$I(\vartheta_i') \approx I_{\rm sp}(\vartheta_i') + I_{\rm bp}(\vartheta_i') U(\vartheta_i' - \tilde{\vartheta}_i) \tag{19}$$

where $I_{\rm sp}(\vartheta_i')$ and $I_{\rm bp}(\vartheta_i')$ represent the saddle-point and branch-point contribution to the integral of (18), respectively. However, a continuous asymptotic expression for $I(\vartheta_i')$ is required since $C$ does not intersect the branch cut.

According to complex function theory, the integral along the SDC, which is approximated in the right-hand side of (19) by the continuous term $I_{\rm sp}(\vartheta_i')$, is discontinuous at $\vartheta_i' = \tilde{\vartheta}_i$, this discontinuity being equal to the integral around the branch cut. Hence, $I_{\rm sp}(\vartheta_i')$ must be augmented with an appropriate discontinuous term $I_d(\vartheta_i')$ to cancel out the discontinuity of $I(\vartheta_i')$, as given by (19).

We consider the general expression $F(a) = F_1(a) + F_2(a)\sqrt{n_i^2 - \sin^2 a}$, where $F_1(a)$, $F_2(a)$ are analytic at $a = a_i$. Close inspection of the integral along the SDC suggests that the aforementioned discontinuity is associated with integration of the singular part of $F(a)$ from $a_0$ to $\pi/2 + \vartheta_i' + j\infty$ (Fig. 7), where $a_0 \to a_i$ as $\vartheta_i' \to \tilde{\vartheta}_i$. Hence, $I_d(\vartheta_i')$ may be expressed as follows:

$$I_d(\vartheta_i') = \int_{a_0}^{\pi/2 + \vartheta_i' + j\infty} F_2(a)\sqrt{n_i^2 - \sin^2 a} e^{-jk_0 R_i' \cos(\vartheta_i' - a)}\, da. \tag{20}$$

We use the approximation $F_2(a)\sqrt{n_i^2 - \sin^2 a} \approx F_2(a_i)\sqrt{-2n_i(a - a_i)\cos a_i}$ in the vicinity of $a_i$; moreover, we introduce the variable $u = -jk_0 R_i'(\cos(\vartheta_i' - a_0) - \cos(\vartheta_i' - a))$, thus transforming (20) into the following:

$$I_d(\vartheta_i') \approx \frac{F_2(a_i)\sqrt{2n_i \cos a_i}\,\mathrm{sgn}(\vartheta_i' - \tilde{\vartheta}_i)}{\sqrt{jk_0^3 R_i'^3}\sin(\vartheta_i' - a_0)\sqrt{\sin(\vartheta_i' - a_i)}} \times e^{-jk_0 R_i' \cos(\vartheta_i' - a_0)} \int_0^\infty \sqrt{u - u_i} e^{-u}\, du. \tag{21}$$

By use of the definition $\Gamma(\alpha, z) = \int_z^\infty e^{-t} t^{\alpha - 1}\, dt$ for the incomplete Gamma function [32] and the approximation $a_0 \approx a_i$, we obtain the asymptotic expression

$$I_d(\vartheta_i') \approx \frac{F_2(a_i)\sqrt{2n_i \cos a_i}\,\mathrm{sgn}(\vartheta_i' - \tilde{\vartheta}_i)}{\sqrt{jk_0^3 R_i'^3 \sin^3(\vartheta_i' - a_i)}} \times e^{-jk_0 R_i' \cos(\vartheta_i' - a_i)} \Gamma(3/2, -u_i). \tag{22}$$

It can be shown that (22) is equivalent to

$$I_d(\vartheta_i') = \frac{1}{\sqrt{\pi}} I_{\rm bp}(\vartheta_i')\,\mathrm{sgn}(\tilde{\vartheta}_i - \vartheta_i')\Gamma(3/2, -u_i) \tag{23}$$

and, if $I_d(\vartheta_i')$, as given by (23), is incorporated in the right-hand side of (19), we obtain

$$I(\vartheta_i') \approx I_{\rm sp}(\vartheta_i') + I_{\rm bp}(\vartheta_i') g(\vartheta_i') \tag{24a}$$

$$g(\vartheta_i') = U(\vartheta_i' - \tilde{\vartheta}_i) + \frac{1}{\sqrt{\pi}}\,\mathrm{sgn}(\tilde{\vartheta}_i - \vartheta_i')\Gamma(3/2, -u_i). \tag{24b}$$

If $\vartheta_i' \to \tilde{\vartheta}_i$, then $u_i \to 0$; since $\Gamma(3/2, 0) = \sqrt{\pi}/2$, $I(\vartheta_i')$, as given by (24a), is continuous at $\vartheta_i' = \tilde{\vartheta}_i$.

So far, we have assumed that $a_0$ is close to $a_i$, which implies that $\vartheta_i'$ is close to $\tilde{\vartheta}_i$; yet, (24) may be used for any $\vartheta_i' \in (0, \pi/2)$, provided that $a_0$ is chosen so that $g(\vartheta_i') \to U(\vartheta_i' - \tilde{\vartheta}_i)$ as $\vartheta_i'$ moves away from $\tilde{\vartheta}_i$. Considering that $\Gamma(3/2, -u_i) \approx e^{u_i}\sqrt{-u_i}$ for large $|u_i|$, $a_0$ must be chosen so that $\mathrm{Re}\, u_i < 0$. Convenient choices for $a_0$ are along the dashed curves that emanate from $a_i$ (Fig. 7); those curves correspond to $\mathrm{Re}\sqrt{n_i^2 - \sin^2 a} = 0$ and $\mathrm{Im}(a - a_i) = \cosh^{-1}(\csc(\mathrm{Re}\, a)) - \cosh^{-1}(\csc(\mathrm{Re}\, a_i))$, for $\vartheta_i' < \tilde{\vartheta}_i$ and $\vartheta_i' > \tilde{\vartheta}_i$, respectively. Furthermore, the preceding analysis, if extended to complex values of $R_i'$ and $\vartheta_i'$ yields the following generalized result:

$$g(\vartheta_i'; R_i') = \alpha(\vartheta_i'; R_i') + \frac{1}{\sqrt{\pi}}\beta(\vartheta_i'; R_i')\Gamma(3/2, -u_i) \tag{25}$$

where $\alpha(\vartheta_i'; R_i') = 1$ or zero, and $\beta(\vartheta_i'; R_i') = -1$ or one, if the SDC does or does not intersect the branch cut, respectively.

## REFERENCES


[1] G. D. Maliuzhinets, "Excitation, reflection and emission of surface waves from a wedge with given face impedances," *Sov. Phys. Dokl.*, vol. 3, pp. 752–755, 1958.

[2] R. Tiberio, G. Pelosi, and G. Manara, "A uniform GTD formulation for the diffraction by a wedge with impedance faces," *IEEE Trans. Antennas Propagat.*, vol. AP-33, pp. 867–873, Aug. 1985.

[3] T. Griesser and C. A. Balanis, "Reflections, diffractions, and surface waves for an interior impedance wedge of arbitrary angle," *IEEE Trans. Antennas Propagat.*, vol. 37, pp. 927–935, July 1989.

[4] S. Sanyal and A. K. Bhattacharyya, "Diffraction by a half-plane with two face impedances, uniform asymptotic expansion for plane wave and arbitrary line source incidence," *IEEE Trans. Antennas Propagat.*, vol. AP-34, pp. 718–723, May 1986.

[5] R. Tiberio, G. Pelosi, G. Manara, and P. H. Pathak, "High-frequency scattering from a wedge with impedance faces illuminated by a line source, part I: Diffraction," *IEEE Trans. Antennas Propagat.*, vol. 37, pp. 212–218, Feb. 1989.

[6] G. Pelosi, R. Tiberio, and R. G. Rojas, "Electromagnetic field excited by a line source placed at the edge of an impedance wedge," *IEEE Trans. Antennas Propagat.*, vol. 39, pp. 1043–1046, July 1991.

[7] G. Manara, R. Tiberio, G. Pelosi, and P. H. Pathak, "High-frequency scattering from a wedge with impedance faces illuminated by a line source—Part II: Surface waves," *IEEE Trans. Antennas Propagat.*, vol. 41, pp. 877–883, July 1993.

[8] M. F. Otero and R. G. Rojas, "Two-dimensional Green's function for a wedge with impedance faces," *IEEE Trans. Antennas Propagat.*, vol. 45, pp. 1799–1809, Dec. 1997.

[9] T. B. A. Senior, "Diffraction tensors for imperfectly conducting edges," *Radio Sci.*, vol. 10, no. 10, pp. 911–919, Oct. 1975.

[10] T. B. A. Senior, "Skew incidence on a right-angled impedance wedge," *Radio Sci.*, vol. 13, no. 4, pp. 639–647, July/Aug. 1978.

[11] T. B. A. Senior, "Solution of a class of imperfect wedge problems for skew incidence," *Radio Sci.*, vol. 21, no. 2, pp. 185–191, Mar./Apr. 1986.

[12] O. M. Bucci and G. Franceschetti, "Electromagnetic scattering by a half-plane with two face impedances," *Radio Sci.*, vol. 11, no. 1, pp. 49–59, Jan. 1976.

[13] J. L. Volakis, "A uniform geometrical theory of diffraction for an imperfectly conducting half-plane," *IEEE Trans. Antennas Propagat.*, vol. AP-34, pp. 172–180, Feb. 1986.

[14] T. B. A. Senior and J. L. Volakis, "Scattering by an imperfect right-angled wedge," *IEEE Trans. Antennas Propagat.*, vol. AP-34, pp. 681–689, May 1986.
[15] R. G. Rojas, "Wiener-Hopf analysis of the EM diffraction by an impedance discontinuity in a planar surface and by an impedance half-plane," *IEEE Trans. Antennas Propagat.*, vol. 36, pp. 71–83, Jan. 1988.
[16] R. G. Rojas, "Electromagnetic diffraction of an obliquely incident plane wave field by a wedge with impedance faces," *IEEE Trans. Antennas Propagat.*, vol. 36, pp. 956–970, July 1988.
[17] G. Pelosi, S. Maci, R. Tiberio, and A. Michaeli, "Incremental length diffraction coefficients for an impedance wedge," *IEEE Trans. Antennas Propagat.*, vol. 40, pp. 1201–1210, Oct. 1992.
[18] C. Demeterscu, "A general solution of the second-order difference equation occurring in diffraction theory," *Radio Sci.*, vol. 31, no. 3, pp. 461–467, May–June 1996.
[19] R. G. Kouyoumjian and P. H. Pathak, "A uniform geometrical theory of diffraction for an edge in a perfectly conducting surface," *Proc. IEEE*, vol. 62, pp. 1448–1461, Nov. 1974.
[20] K. A. Chamberlin and R. J. Luebbers, "An evaluation of Longley–Rice and GTD propagation models," *IEEE Trans. Antennas Propagat.*, vol. AP-30, pp. 1093–1098, Nov. 1982.
[21] W. D. Burnside and K. W. Burgener, "High frequency scattering by a thin lossless dielectric slab," *IEEE Trans. Antennas Propagat.*, vol. AP-31, pp. 104–110, Jan. 1983.
[22] R. J. Luebbers, "Finite conductivity uniform GTD versus knife edge diffraction in prediction of propagation path loss," *IEEE Trans. Antennas Propagat.*, vol. AP-32, pp. 70–76, Jan. 1984.
[23] C. S. Joo, J. W. Ra, and S. Y. Shin, "Scattering by right angle dielectric wedge," *IEEE Trans. Antennas Propagat.*, vol. AP-32, pp. 61–69, Jan. 1984.
[24] S. Y. Kim, J. W. Ra, and S. Y. Shin, "Diffraction by an arbitrary-angled dielectric wedge: Part I—Physical optics approximation," *IEEE Trans. Antennas Propagat.*, vol. 39, pp. 1272–1281, Sept. 1991.
[25] S. Y. Kim, J. W. Ra, and S. Y. Shin, "Diffraction by an arbitrary-angled dielectric wedge: Part II—Correction to physical optics solution," *IEEE Trans. Antennas Propagat.*, vol. 39, pp. 1282–1292, Sept. 1991.
[26] L. M. Brekhovskikh, *Waves in Layered Media*. New York: Academic, 1960.
[27] R. J. Luebbers, "Comparison of lossy wedge diffraction coefficients with application to mixed path propagation loss prediction," *IEEE Trans. Antennas Propagat.*, vol. 36, pp. 1031–1034, July 1988.
[28] A. Ishimaru, *Electromagnetic Wave Propagation, Radiation, and Scattering*. Englewood Cliffs, NJ: Prentice-Hall, 1991.
[29] A. Baños Jr., *Dipole Radiation in the Presence of a Conducting Half-Space*. Oxford, U.K.: Pergamon, 1966.
[30] J. A. Stratton, *Electromagnetic Theory*. New York: McGraw-Hill, 1941.
[31] L. B. Felsen and N. Marcuvitz, *Radiation and Scattering of Waves*. Englewood Cliffs, NJ: Prentice-Hall, 1973.
[32] M. Abramowitz and I. A. Stegun, *Handbook of Mathematical Functions*. New York: Dover, 1970.

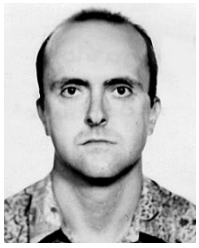

**Athanasios I. Papadopoulos** (S'94) received the M.Sc. degree from the Department of Electrical and Computer Engineering, Faculty of Technology, Aristotle University of Thessaloniki, Greece, in 1992. He is currently working toward the Ph.D. degree at the same university.

His research interests are in the areas of electromagnetic wave propagation and scattering as well as in the diffraction of electromagnetic waves by gratings and wedges.

Mr. Papadopoulos is a a member of the Technical Chamber of Greece.

**Dimitrios P. Chrissoulidis** (S'78–M'84) was born in Thessaloniki, Greece, in 1956. He received the M.Sc. and Ph.D. degrees from the Department of Electrical and Computer Engineering, Faculty of Technology, Aristotle University of Thessaloniki, Greece, in 1979 and 1984, respectively.

In 1988, he was a Postdoctoral Fellow of the Environmental Surveillance Technology Programme, Royal Norwegian Council for Scientific and Industrial Research, Kjeller, Norway. Currently, he is an Associate Professor in the Department of Electrical and Computer Engineering, Faculty of Technology, Aristotle University of Thessaloniki, Greece. He is also Director of the Telecommunications Division of the same university and Coordinator of the Radar and Microwaves Unit of the Telecommunications Laboratory. His research interests are in the areas of electromagnetic wave propagation and scattering, microwave remote sensing of the environment, and underwater acoustics.

Dr. Chrissoulidis is a member of the AGU, URSINF, and of the Technical Chamber of Greece.